

---

## Contributi scientifici dei vincitori dei premi di partecipazione SISM al Multinational Congress on Microscopy 2019

### Scientific contributions by the winners of the Italian Society for Microscopical Sciences participation awards to the 2019 Multinational Congress on Microscopy

In occasione del 14<sup>th</sup> Multinational Congress on Microscopy, che si è tenuto a Belgrado dal 15 al 20 settembre 2019, la SISM ha bandito dieci premi, dell'importo di 500 Euro ciascuno, per favorire la partecipazione al congresso di ricercatori non strutturati.

Il Consiglio Direttivo, sulla base della valutazione degli *abstract* inviati al MCM 2019 e del *curriculum vitae*, ha stilato una graduatoria e selezionato i dieci vincitori, tutti giovani Soci SISM che svolgono la loro attività di ricerca nel campo delle Scienze Biomediche o della Scienza dei Materiali: Debora Burini (Università di Urbino), Flavia

Carton (Università di Verona), Manuela Costanzo (Università di Verona), Gloria D'Avack (Istituto Superiore di Sanità), Paolo D'Incecco (Università di Milano), Francesco Garzella (Istituto Italiano di Tecnologia di Genova e Università di Parma), Daniel Knez (CNR, Trieste), Laura Pagliari (Università di Udine), Paolo Rosi (Università di Modena e Reggio Emilia), Sara Salucci (Università di Urbino).

I contributi di seguito pubblicati descrivono i risultati scientifici presentati dai vincitori al MCM 2019 e testimoniano la qualità del loro lavoro sperimentale.

## DEXAMETHASONE-INDUCED MUSCLE FIBER ATROPHY: MAY A NATURAL ANTIOXIDANT PREVENT IT?

D. Burini, S. Burattini, D. Curzi, G. Zappia, P. Gobbi, E. Falciari, S. Salucci

Department of Biomolecular Sciences, University of Urbino, Urbino, Italy

E-mail: debora.burini@uniurb.it

Muscle disorders may occur under different physiological conditions, such as severe injury, sedentariness, aging, hormone imbalances, cancer and excessive oxidative stress<sup>1</sup>. This latter has a significant role in mitochondrial damage, which contributes to muscle atrophy onset<sup>2</sup>. One of the causes of increased oxidative stress is a prolonged exposure to anti-inflammatory drugs, whose effects may be limited by some natural antioxidants<sup>3</sup>, which could be used as a potential therapeutic intervention in some muscle diseases.

In our study, we have evaluated the possible protective effects of a virgin oil flavonoid, a natural antioxidant not extensively studied in muscle tissue, in C2C12 myotubes treated with Dexamethasone, a common glucocorticoid used to mimic muscle wasting *in vitro*. Some myotubes were fixed and observed by environmental scanning electron microscopy and transmission electron microscopy. The remaining live cells have been treated with JC1, a fluorochrome for mitochondrial membrane potential monitoring, and analyzed with confocal laser scanning microscopy (CLSM). Control cells, which appear aligned and elongated, reveal a healthy ultrastructure of mitochondria and myonuclei. On the contrary, fibers treated with glucocorticoid appear smaller and show chromatin condensation, membrane blebs and altered or empty mitochondria, with a loss of membrane potential. Finally, myotubes treated with the antioxidant before drug administration appear comparable to the control ones, showing preserved fibers and mitochondria, as demonstrated at CLSM too.

Therefore, our preliminary data display that this natural antioxidant seems to have a protective effect in Dexamethasone-induced C2C12 myotubes atrophy, preventing or limiting muscle mass reduction and cell damage.

### References

1. Cohen S, et al. *Nat Rev Drug Discov* 2015, 14:58-74.
2. Salucci S, et al. *Microsc Res Tech* 2017, 80:1174-81.
3. Salucci S, et al. *Eur J Histochem* 2017, 61:2784.

## ALCIAN BLUE STAINING TO VISUALIZE HYALURONIC-ACID BASED NANOPARTICLES AT TRANSMISSION ELECTRON MICROSCOPY

F. Carton<sup>1,2</sup>, M. Repellin<sup>1,2</sup>, G. Lollo<sup>2</sup>, M. Malatesta<sup>1</sup>

<sup>1</sup>Department of Neurosciences, Biomedicine and Movement Sciences, Anatomy and Histology Section, University of Verona, Italy; <sup>2</sup>Laboratory of Automatic Control, Chemical and Pharmaceutical Engineering, University of Lyon, France.

E-mail: flavia.carton@univr.it

In recent years, a lot of work has been done to develop nanostructured materials as drug delivery systems for biomedical applications. Investigating the interaction of nanoparticles (NPs) with cells and tissues is mandatory to select appropriate biocompatible nanocarriers. Thanks to its high resolution, transmission electron microscopy (TEM) is a suitable technique for detecting NPs and tracking their fate inside the cells<sup>1</sup>. This is relatively easy for NPs that contain electron dense constituents such as metal ions; on the contrary, NPs made of organic components (*e.g.* lipids or polymers) are moderately electron-dense, thus often being hardly discernable in the cytosolic milieu. In a previous study, we solved this problem by labelling organic NPs with fluorochromes during the synthetic procedure, and then applying the technique of diaminobenzidine photo-oxidation: by this method, the fluorescent signal is converted into a finely granular electron-dense product thus making NPs unequivocally detectable at TEM<sup>2</sup>. Unfortunately, this technique cannot be applied in the presence of a marked fluorescence background, as we found with hyaluronic acid (HA)-based NPs (HA-NPs)<sup>3</sup>. To overcome this problem, we set up an alternative detection method using the long established critical-electrolyte-concentration technique applied to the Alcian Blue (AB) staining<sup>4</sup>.

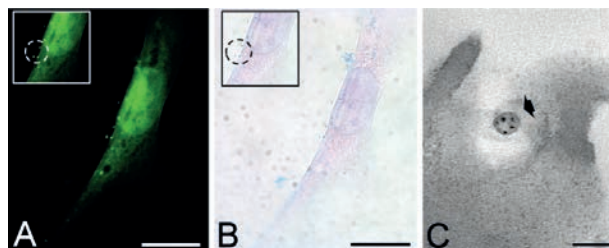


**Figure 1.** Micrographs at fluorescence (A) and bright field (B) microscopy of a C2C12 myoblasts incubated with FITC-labelled HA-NPs for 48 h and then stained with AB. HA-NPs are clearly recognizable at the surface and inside the cells both as green fluorescent spot (A, inset) and as blue dots (B, inset). TEM micrograph (C) of a HA-NP (arrowhead) occurring in a plasma membrane invagination; note the granular electron-dense product of AB staining. Bars: 20  $\mu$ m (A,B); 100 nm (C).

C2C12 murine myoblasts were seeded on glass coverslips and grown in Dulbecco's modified Eagle medium. The cells were then treated with either HA-NPs or FITC-labelled HA-NPs for TEM and bright field/fluorescence microscopy, respectively. After aldehyde fixation, the cells were stained following the method described by Schofield *et al.*<sup>5</sup>. The samples were then processed for observation at bright field and fluorescence microscopy or at TEM.

Following AB staining, fluorescently-labelled HA-NPs (that are visualized as green spots in fluorescence microscopy) appear as blue dots in bright field microscopy: this was observed with both HA-NPs in suspension and after their internalization in cultured cells, where the co-localization of the green and blue signals confirmed the reaction of AB with HA (Figure 1A,B). At TEM, the AB staining appears as a granular electron-dense product (Figure 1C), as already observed by Schofield *et al.* in cartilage samples<sup>5</sup>. No reaction was found on any cellular components, thus confirming the specificity of AB for HA.

AB staining proved to be a simple and reliable method to visualize HA-NPs in cultured cells after the usual procedures of fixation and embedding for TEM. The possibility to stain fluorescently labelled HA-NPs with AB allows to foresee the application of this staining technique also in correlative microscopy.

## References

1. Repellin M, Carton F. *Microscopie* 2019, 30(1):8-14.
2. Malatesta M, et al. *Eur J Histochem* 2012, 56:e20.
3. Oyarzum-Ampuero FA, et al. *Eur J Pharm Biopharm* 2011, 79:54-7.
4. Scott JE, et al. *Histochemie* 1965, 5:221-3.
5. Schofield BH, et al. *Histochem J* 1975, 7:139-49.

## NANOCARRIERS FOR SKELETAL MUSCLE THERAPY: TESTS *IN VITRO* ON CELL AND ORGAN MODELS

M. Costanzo<sup>1</sup>, F. Vurro<sup>1</sup>, L. Calderan<sup>1</sup>, F. Boschi<sup>2</sup>, I. Andreana<sup>3</sup>, S. Arpicco<sup>3</sup>, B. Stella<sup>3</sup>, M. Malatesta<sup>1</sup>

<sup>1</sup>Department of Neurosciences, Biomedicine and Movement Sciences, University of Verona, Verona, Italy; <sup>2</sup>Department of Computer Science, University of Verona, Verona, Italy;

<sup>3</sup>Department of Drug Science and Technology, University of Turin, Torino, Italy

E-mail: manuela.costanzo@univr.it

Myotonic dystrophy (DM) is a genetically-based neuromuscular disorder characterized by a variety of multisystemic features including myotonia, muscular dystrophy, dilated cardiomyopathy<sup>1</sup>. No therapies are currently available for DM: in fact, therapeutic molecules that were successfully tested in experimental models *in vivo* and *in vitro* proved to be hardly useful for humans because of their low

bioavailability, due to enzymatic degradation or high systemic toxicity.

Nanocarriers have become popular in the biomedical field thanks to their ability to protect encapsulated molecules from enzymatic degradation, and to their potential as drug-delivery systems for controlled and targeted drug release inside the cells<sup>2</sup>: thus nanocarriers -among which Liposomes (LPs) and Poly Lactic-co-Glycolic Acid nanoparticles (PLGA NPs)- are potentially appropriate tools for delivering drugs to diseased muscle cells.

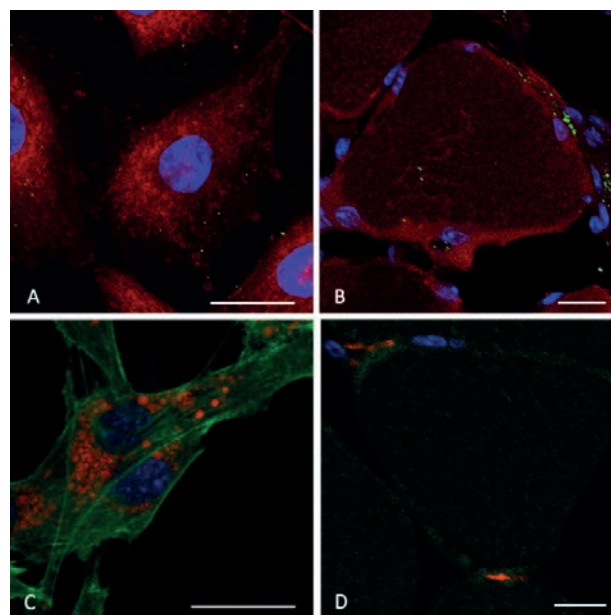


**Figure 1.** Confocal optical sections of C2C12 myoblast 24 h after incubation (A and C) and cross sections of soleus muscles 1 h post-intramuscular injection (B and D). A,B: FITC-labelled LPs (green fluorescence); the cytoplasm was counterstained with trypan blue. C,D: Nile red-labelled PLGA NPs (red fluorescence); the cytoplasm was counterstained with FITC. The cell nuclei were stained for DNA with Hoechst 33342 (blue fluorescence). Bars: 25  $\mu$ m.

As a preliminary step toward a therapy for DM, here we investigated by confocal fluorescence microscopy (CFM) and transmission electron microscopy (TEM) the uptake and the distribution of LPs and PLGA NPs in skeletal muscle cells using two different experimental murine models *in vitro*: C2C12 cells and explanted soleus muscles. C2C12 cells are immortalized murine myoblasts that spontaneously differentiate into myotubes in low-serum containing media, thus providing an *in vitro* model of both proliferating and terminally differentiated non-cycling muscle cells. Both LPs and PLGA NPs proved to be biocompatible for C2C12 cycling myoblasts and non-cycling myotubes. The nanocar-

riers were labelled with either fluorescein isothiocyanate, FITC (LPs) or Nile red (PLGA NPs) to make them visible at CFM (Figure 1A-D). In C2C12 myoblasts, LPs occurred as isolated fluorescing spots in the peripheral cytoplasmic region (Figure 1A), whereas PLGA NPs accumulated in large amount and, usually, as aggregates in the perinuclear area of the cytoplasm (Figure 1C). Both nanocarriers were never observed inside the nucleus. LPs were less efficiently internalized than PLGA NPs, in both myoblasts and myotubes, while the internalization of both nanocarriers was lower in the myotubes than in the myoblasts<sup>3</sup>. TEM showed that LPs enter the cells by fusion with the plasma membrane and rapidly disaggregate in the cytoplasm, their remnants migrating through the cytosol toward the lipid droplets. PLGA NPs are internalized by endocytosis and rapidly undergo endosomal escape into the cytosol; however, they may re-enter the lytic pathway *via* autophagy.

As a second step, we investigated the biodistribution of LPs and PLGA NPs in explanted mouse skeletal muscles maintained in a novel *in vitro* fluid dynamic system able to improve the structural preservation of explanted mouse skeletal muscle<sup>4</sup>. Fluorescent nanocarriers were injected into the muscle, and their biodistribution was monitored in cryosections by CFM. LPs did enter myofibres, although being partially entrapped in the connective tissue (Figure 1B). On the contrary, PLGA NPs were only found in the perimysium and endomysium, but never inside the muscle fibres (Figure 1D). Further studies are in progress to functionalize the nanocarriers in the attempt to improve their targeting to the myofibres in explanted muscles.

The observed differences in the uptake of LPs and PLGA NPs in the two different *in vitro* models highlight that conventional cell cultures are useful for testing the suitability of nanocarriers in the early research phase, but investigations of their effect in tissues and organs from biopsies or surgical material are more appropriate to mimic their actual behaviour *in vivo*.

#### References

1. Harper PS. "Myotonic Dystrophy" London: WB Saunders 2001.
2. Dilnawaz F, et al. Int J Pharm 2018, 538:263-78.
3. Costanzo M, et al. Nanomedicine 2019, 14:301-16.
4. Carton F, et al. Eur J Histochem 2017, 61:2862.

## ELECTROPORATION: NEW STRATEGY TO IMPROVE THE DRUG UPTAKE AND OVERCOME THE TUMOR RESISTANCE

M. Condello, G. D'Avack, S. Meschini

National Center for Drug Research and Evaluation, Istituto Superiore di Sanità, Rome, Italy

E-mail: gloria.davack@gmail.com

Electrochemotherapy is an innovative therapeutic strategy to overcome multidrug resistance (MDR) phenomenon of several neoplasms. New anticancer treatment combines the administration of a chemotherapeutic agent with the application of electric pulses (electroporation, EP) having appropriate waveforms to increase drug uptake. Its efficacy, as adjuvant therapy, has already been demonstrated in the veterinary patients, in combination with several anticancer agents resulting in enhanced cytotoxicity. The main goal of our project is to increase the effectiveness of doxorubicin (DOX) on MDR human colon adenocarcinoma cell line (LoVo DX) and mitomycin C (MMC) on two human breast adenocarcinoma cell lines (MCF-7 WT and MCF-7 DX), by using trains of biphasic pulses. The *in vitro* experiments of the combined treatment (EP plus DOX) showed the enhancement of DOX accumulation and nuclear distribution on LoVo DX cell suspension, evaluated by flow cytometry and confocal microscopy, respectively. Moreover, evident morphological changes were observed by scanning electron microscopy. MTT assay showed that MCF-7 cells treated with electroporation alone, showed the same cell viability as the control; this proves that electrical impulses alter only the membrane permeability favouring drug uptake without inducing a cytotoxic effect on tumor cells. Cell viability assay showed a 20% reduction after the combined EP plus MMC treatment. Further studies will be carried out to confirm the cytotoxic damage and assess the role of electrochemotherapy in the pharmacological resistance phenomenon.

## MICROSCOPY APPLICATIONS IN FOOD SCIENCE FOR A DEEP INVESTIGATION OF DAIRY PRODUCT SPOILAGE

P. D'Incecco, V. Rosi, L. Pellegrino

Department of Food, Environmental and Nutritional Sciences, University of Milan, Milan, Italy

E-mail: paolo.dincecco@unimi.it

Spoilage of food products still represents a problem for manufacturers because it may cause consumer complaints and product recall. Two case studies that represent big issues to dairy manufactures are here presented: the late blowing defect affecting extra-hard cheeses and the instability of

UHT milk during its shelf life. Due to the complexity of these topics and the number of involved aspects, the usual chemical analyses were successfully combined with different microscopy evaluations.

**Case Study 1.** The late blowing is the most devastating defect that may affect hard cheeses such as Grana Padano (GP) and Parmigiano-Reggiano (PR). It implies the formation of openings and holes within the cheese, sometimes accompanied by cracks, due to the butyric acid fermentation caused by some species of spore-former Clostridia, mostly *Clostridium tyrobutyricum*. Growth of these bacteria occurs during the cheese ripening, when the conditions progressively become favourable to both spore germination and the development of vegetative cells<sup>1</sup>.

Natural creaming of raw milk is the first step of the consolidated cheese making of GP and PR during which fat globules rise to the top of the milk together with spores, vegetative cells and somatic cells. Thus, the skimming and heating of milk take place at the same time<sup>2</sup>. Spores remaining in the milk will be entrapped in the curd and eventually cause insurgence of the defect. Milk immunoglobulins (Igs) have been indicated as one of the factors necessary for the removal of bacterial spores from milk by natural creaming but their specific role has not been clarified yet. We have therefore performed an ultrastructural study to investigate the behaviour of fat globules and their interactions with bacterial cells or spores during raw milk creaming. Interactions between fat globules and spores were best investigated by transmission electron microscopy (TEM) with prior resin embedding. Spores attached to fat globules membrane through an electron-opaque material, where presence of individual Igs classes (IgA, IgM, IgG) was identified by means of post immunogold labelling. This study showed that interaction of cells and spores of Clostridia with fat is Igs-mediated and thus the level of native Igs in milk is crucial for the efficiency of their removal.

**Case study 2.** UHT milk is the most commercialized milk worldwide because of its storage stability at non-refrigerated condition for 3-6 months. However, two main types of instability may occur during the shelf storage of this product: creaming of fat at the top of the milk and gelation of protein components. The insurgence of both phenomena often implies the recall of the product from the market and thus a food waste. Understanding promoting conditions and initiating mechanisms of these phenomena is thus essential to find out suitable technological strategies for prevention. A high-pressure double homogenization of milk delayed appearance of a visible cream layer in the packaged milk up to 12 months. Confocal laser scanning microscopy (CLSM) and TEM analyses showed that this innovative process not only decreased fat globule size, compared with the conven-

tional single process, but also increased the interactions between fat globule membrane and casein micelles with formation of high-density aggregates that prevent creaming of fat globules.

Gelation of UHT milk is caused by proteolytic activity of heat-resistant enzymes from different strains of *Pseudomonas* spp. on casein (3). To simulate gelation at lab scale, milk was inoculated with three strains of *Pseudomonas* and test samples were stored at 25 or 40°C up to 90 days. Activity of heat-resistant enzymes was monitored by capillary electrophoresis and HPLC-MS. Caseinomacropeptides (CMPs), released from k-casein by specific proteases, were detected in sterilized milk well before gelation onset and accumulated during storage. In parallel, changes in the microstructure of milk were monitored by CLSM. We observed a progress in the aggregation of protein while the content of CMPs increased (Fig. 1). Thus, CMPs were proposed as marker for an early detection of UHT milk gelation.

In conclusion, microscopy has a key role in understanding the effects of process technologies on food structure and on interaction or stability of food components. Moreover, as shown in these studies, a multidisciplinary approach may allow a complete characterization of the food matrix, which is essential for the comprehension of mechanisms involved in the food spoilage phenomena.

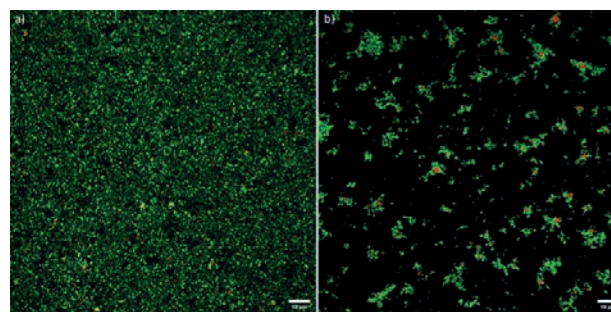


**Figure 1.** Microstructure of stable (a) and unstable (b) milk due to bacterial enzymatic activity.

#### References

1. Ávila M, et al. Food Microbiol 2016, 60:165-73.
2. D'Incecco P, et al. J. Dairy Sci 2015, 98:5164-72.
3. Anema SG. Compr Rev Food Sci Food Saf 2019, 18:140-66.

## PHOTOCHROMIC MOLECULAR PROBES FOR PHOTOACOUSTIC MICROSCOPY

F. Garzella<sup>1,2</sup>, C. Viappiani<sup>2</sup>, R. Bizzarri<sup>4</sup>, B. Storti<sup>4</sup>, S. Abbruzzetti<sup>2</sup>, A. Losi<sup>2</sup>, W. Gärtner<sup>5</sup>, P. Bianchini<sup>1</sup>, A. Diaspro<sup>1,3</sup>

<sup>1</sup>Nanoscopy and NIC@IIT, Istituto Italiano di Tecnologia, Genova, Italy; <sup>2</sup>Department of Mathematical, Physical and Computer Sciences, University of Parma, Parma, Italy; <sup>3</sup>Department of Physics, University of Genova, Genova, Italy; <sup>4</sup>NEST, Scuola Normale Superiore and NANO-CNR, Pisa, Italy; <sup>5</sup>Institute for Analytical Chemistry, University of Leipzig, Leipzig, Germany

E-mail: francesco.garzella@iit.it

The photoacoustic effect (PA) is a physical phenomenon involving the generation of sound waves following light absorption in a material sample. The generation of sound waves follows the irradiation of light absorbing systems: photon absorption and subsequent non-radiative relaxation of the chromophores induces a rapid rise in temperature within the sample. This isochoric heating raises the pressure within the sample by  $\Delta p = \Gamma \mu_a F$ , where  $\Gamma$  is the Grüneisen parameter,  $\mu_a$  is the optical absorption coefficient, and  $F$  is the incident laser fluence. This pressure rise induces a thermoelastic expansion, and the emission of a pressure wave called a photoacoustic wave. Nowadays the implementation of photoacoustic microscopy techniques (PAM) has completely improved our way of obtaining *in vivo* images. Depending on what drives the spatial resolution of the method, the diameter of the laser beam or the transducer focal spot, we divide PAM into optical-resolution photoacoustic microscopy (OR-PAM), acoustic-resolution microscopy (AR-PAM)<sup>1</sup>.

The base of the contrast in photoacoustic imaging is the different absorption coefficients of tissue components like blood, melanin, and lipids or suitable transgene labels in the sample. However, the low number of transgene probes and their poor signal generation efficiency for photoacoustic imaging limits studies of living animals and processes at the cellular and subcellular levels. The relatively weak photoacoustic signals generated by illuminating transgene labels at single wavelengths results in weak contrast compared to other strong absorbers like hemoglobin or melanin. Reversibly switchable fluorescent proteins (rsFPs) have had a revolutionizing effect on life science imaging due to their contribution to sub-diffraction-resolution optical microscopy (nanoscopy) as agents able to improve contrast-to-noise ratio and spatial resolution<sup>2</sup>. However, rsFPs show different photophysical behavior in PA than in optical microscopy because PA requires pulsed illumination and depends on signal generation *via* nonradiative energy decay channels and this implies that rsFPs optimized for fluores-

cence imaging may not be ideal for PA since light emission and heating are competitive processes in depleting excited states energy<sup>3</sup>.

The main aim of this project is the development and study of novel photochromic proteins for photoacoustic microscopy characterized by a lower fluorescence quantum yield in comparison to available rsFPs. In particular, we considered two different families of photochromic proteins: GAF3<sup>4</sup>, and two novel mutants of GFPs obtained adding a fluorescence-decreasing mutation to wildQ and wildQT proteins<sup>5</sup>.

GAF3 is the third domain of the protein encoded by the gene *slr1393* from the cyanobacterium *Synechocystis sp.* PCC6803 (Slr1393) and the sole domain showing photochromism, by switching between a red-absorbing parental state (GAF3R,  $\lambda_{\max} = 649$  nm) and a green-absorbing photo-product state (GAF3G,  $\lambda_{\max} = 536$  nm) upon appropriate irradiation (figure 1 left). The protein has been tested in a pump and probe system showing a good difference between the peaks height of two forms at 532 nm pulse excitation wavelength which, due to the strong absorption of the red form in the region of the spectrum of the green form, is the one showing lower contrast (figure 1 right). WildQ and wildQT, respectively E222Q wtGFP and E222Q EGFP, have been used as a starting point for rational mutagenesis involving the addition of Y145W, which is supposed to substantially decrease fluorescence quantum yield. The proteins display the predicted behavior with a fluorescence quantum yield which respectively for low-wildQ and low-wildQT the 20% and 10% of the original wildQ protein.

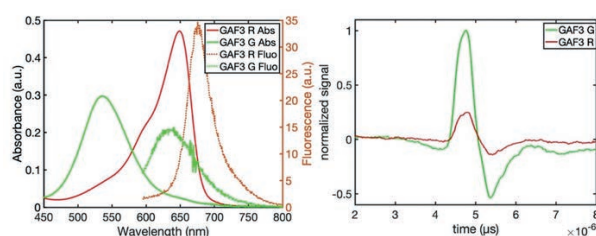


**Figure 1. Left: Absorption and emission spectra of GAF3 protein in red and green forms. Right: Photoacoustic signal of GAF3 protein in red and green form.**

### References

1. Strohm EM, et al. IEEE J Sel Top Quantum Electron 2016, 22:137-51.
2. Vetschera P, et al. Anal Chem 2018, 90:10527-35.
3. Gensch T, Viappiani C. Photochem Photobio. Sci 2003, 2:699-721.
4. Pennacchietti F, et al. Photochem Photobiol Sci 2015, 14:229-37.
5. Storti B, et al. ACS Chem Biol 2018, 8:20182-93.

## IMPACT OF OXYGEN VACANCIES ON ELECTRONIC PROPERTIES OF ANATASE THIN FILMS

D. Knez<sup>1</sup>, G. Dražič<sup>2</sup>, S.K. Chaluvadi<sup>1</sup>, P. Orgiani<sup>1</sup>, R. Ciancio<sup>1</sup>

<sup>1</sup>Istituto Officina dei Materiali-CNR, Trieste, Italy; <sup>2</sup>Laboratory for Materials Chemistry, National Institute of Chemistry, Ljubljana, Slovenia

E-mail: knez@iom.cnr.it

TiO<sub>2</sub> in the anatase crystallographic form is one of the most prominent representatives of the material class of Transition Metal Oxides. These materials find wide application in optoelectronics and photo-electrochemistry, due to their optical properties, catalytic activity and electrochemical stability. Even though anatase is a wide band gap semiconductor with an optical band gap of 3.2 eV, the presence of Ti<sup>3+</sup> localized states, triggered by intrinsic defects, dopants or photoexcitation, extends light absorption into the visible range<sup>1,2</sup>. Thus, tailoring of the optical properties of anatase is of high technological relevance.

A dispersion-less in-gap state can be found after introduction of oxygen vacancies, which generate excess electrons. Interestingly, a red-shift of this state has been observed in highly oxygen deficient TiO<sub>2</sub> films with respect to poorly de-oxygenated ones<sup>2</sup>. Although it is likely that such electronic states originate from structural changes within the TiO<sub>2</sub> films, the exact mechanisms are not yet understood<sup>3</sup>.

Here we study anatase thin films with regard to their structure and morphology and elucidate the influence on electronic properties. The thin films are grown epitaxially by Pulsed Laser Deposition (PLD) on LaAlO<sub>3</sub> substrates with (001) crystallographic orientation. To obtain structural information we apply different transmission electron microscopy (TEM) techniques. Phase contrast in bright field (BF) TEM (Figure 1a) reveals the presence of [103] ordered arrays of defects in the film which are related to the formation of Ti<sub>n</sub>O<sub>2n-1</sub> superstructures originating from the occurrence of oxygen vacancies within the film<sup>4</sup>. We find a typical distance between these vacancies arrays of approximately 1.5 nm. This value is independent of the oxygen vacancy concentration, within the analyzed vacancy concentration range of 5 to 12%.

The presence of a regular structural rearrangement is also confirmed by selected area electron diffraction (SAED, inset of Figure 1a), showing the presence of extra spots superimposed to the characteristic anatase [010] SAED (see arrowed spots in the Figure). Note that the present pattern is acquired from an area larger than the film and, therefore, also shows diffraction spots corresponding to the perovskite-structure of the substrate. The alignment of both patterns demonstrates a good match between substrate and film.

The defect arrays are visible also in scanning TEM (STEM) annular BF (ABF) and, due to the low vacancy concentration, are barely visible in high-angle annular dark-field (HAADF) (Figure 1b). Column-wise integration of the HAADF signal, however, allowed to identify significant intensity variations within the dumbbells, which can be related to local rearrangements of the Ti cations due to the presence of oxygen vacancies (Figure 1c-d). We suggest that stress within the crystal, which is induced by such local atomic displacements, eventually leads to the periodic arrangement of the oxygen vacancies.

We support our results with multislice simulations based on structures obtained from atomistic calculations, such as Molecular Dynamics and Density Functional Theory. Furthermore, we apply electron loss near edge structure (ELNES) studies and correlative spectroscopic techniques available at the APE beamline at Elettra synchrotron.

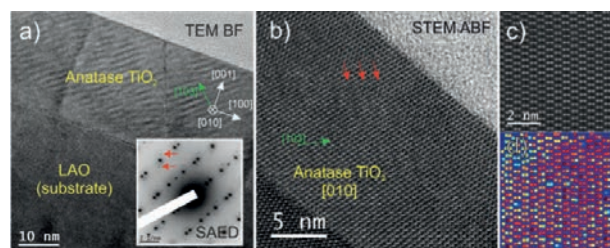


**Figure 1.** a) TEM BF micrograph of the anatase film in [010] zone axis, inset shows the corresponding SAED pattern. Satellite spots caused by the superstructure are indicated by red arrows. b) STEM ABF image showing slight contrast variations in [103] direction. c) Intensity variations, especially between two dumbbell sites can be seen after column-wise intensity integration of the HAADF signal.

### References

1. Zuo F, et al. *J Am Chem Soc* 2010, 132:11856-7
2. Gobaut B, et al. *ACS Appl Mater Interfaces* 2017, 9:23099-106
3. Orgiani P, et al. in preparation
4. Ciancio R, et al. *Phys Rev B* 2012, 86:104110

## GIMME SHELTER: GRAPEVINE PINOT GRIS VIRUS IN DEFORMED ENDOPLASMIC RETICULUM

L. Pagliari<sup>1</sup>, G. Tarquini<sup>1</sup>, S. Buoso<sup>1</sup>, A. Loschi<sup>1</sup>, P. Ermacora<sup>1</sup>, G. Kapun<sup>2</sup>, R. Musetti<sup>1</sup>

<sup>1</sup>Department of Agricultural, Food, Environmental and Animal Sciences, University of Udine, Udine, Italy; <sup>2</sup>Center of Excellence on Nanoscience and Nanotechnology - Nanocenter, Ljubljana, Slovenia

E-mail: laura.pagliari@uniud.it

Grapevine Pinot gris virus (GPGV) is a positive-sense single-stranded RNA [(+)ssRNA] virus often associated to grapevine Pinot gris (GPG) disease. TEM observations allow us to detect the virus in the bundle sheath cells (BSCs) of the infected grapevines, inside uncharacterized membrane-bound structures<sup>1</sup>. It is well known that most of the (+)ssRNA viruses modify host-cell membranes, forming inclusion bodies named viral replication complexes (VRCs). VCRs facilitate viral access to essential host resources and shelter viral genome replication from host antiviral defenses, resulting in optimal environments for viral RNA synthesis<sup>2</sup>. Even if plant viruses can exploit a variety of host cell endomembranes to originate VRCs, most of (+) ssRNA viruses studied usurp the endoplasmic reticulum (ER)<sup>3</sup>. Considering GPGV, the morphology of the altered structures observed in BSCs of GPGV-infected grapevines<sup>1</sup> reminded deformed ER<sup>4</sup>. This hint finds a support in the association of the replicase protein with the host-cell ER reported for grapevine rupestris stem pitting-associated virus (GRSPaV), a virus belonging to the same family of GPGV, *i.e.* the Betaflexiviridae family<sup>3</sup>. In the present study, the identity of the GPGV-induced membranous structures was investigated combining different microscopy techniques and molecular analysis.

The possible interference of GPGV in plant ER-related pathways was investigated considering the expression of genes known to be induced by ER stress<sup>5</sup>. *CALRETICULIN 3* (*CRT3 $\alpha$* , XM\_010652325.2, and *CRT3 $\beta$*  XM\_010650921.2), *CALNEXIN* (*CNX $\alpha$* , XM\_002273672.4, and *CNX $\beta$* , XM\_002277630.4) and *LUMINAL BINDING PROTEIN 5* (*BIP5 $\alpha$* , XM\_002263287.3, and *BIP $\beta$* , XM\_010664593.2) were thus chosen as marker of the possible GPGV-destabilizing interference on ER. Following GPGV infection the expression of all the examined genes, except for *CRT3 $\alpha$* , showed a significant up-regulation.

London Resin White (LRW)-embedded grapevine leaf samples were processed for immunogold analyses. Luminal-binding protein antibody (anti-Bip) localized its target protein not only, as expected, in correspondence to ER in BSCs of healthy plants but also in the membrane-bound structures in BSCs of GPGV-infected samples (Figure 1). Moreover,

antibody directed against double-stranded RNA (anti-dsRNA) failed to mark ER in healthy plants but localized the intermediate of the viral replication only in correspondence to the putative deformed ER. Other cell compartments in infected BSCs were not interested by the anti-dsRNA labelling. Ion beam scanning electron microscopy (FIB-SEM) analysis was performed and 3D datasets were acquired.

To conclude, the use of specific plant ER and viral antibodies combined with TEM gold labeling technique allowed us to confirm the interaction between GPGV and ER in the BSCs. In particular, the association of the viral replication intermediate ds-RNA with the ER-derived structures indicated that GPGV exploits and deforms ER for its replication. The functional relationship between the virus and the plant ER was also assessed by the up-regulation of the expression of different ER-stress related genes in infected plants. FIB-SEM investigation revealed the 3D organization of the ER-derived structures and their connections with the cytoplasmic environment. Besides providing functional information about the still poor investigated GPGV-grapevine interaction, our results aim to help to achieve a better understanding of the microenvironment organization of grapevine viral replication complexes in their natural host.

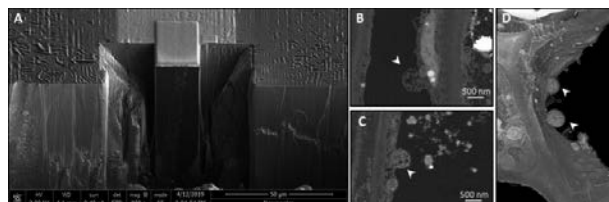


**Figure 1.** FIB-SEM analysis. **A:** individuation of the region of interest for FIB-SEM observations. **B-C:** individuation for the membrane bound structures. **D:** 3D reconstruct.

### References

1. Tarquini G, et al. *Protoplasma* 2018, 255:923-35.
2. Heinlein M. *Virology* 2015 479-480:657-71.
3. Prosser SW, et al. *J Gen Virol* 2015, 96:921-32.
4. Jiang J, et al. *J Virol* 2015 89:6695-710.
5. Liu J-X, Howell SH. *New Phytol* 2016, 211:418-28.
6. Tarquini G, et al. *PLOS ONE* 2019, 14:e0214010.

## TOWARD AN ELECTROSTATIC ORBITAL ANGULAR MOMENTUM SORTER

P. Rosi<sup>1</sup>, A. Tavabi<sup>2</sup>, A. Roncaglia<sup>4</sup>, G. Pozzi<sup>2</sup>, E. Rotunno<sup>3</sup>, M. Zanfrognini<sup>3</sup>, S. Frabboni<sup>1</sup>, R.D. Burkoski<sup>2</sup>, V. Grillo<sup>1,3</sup>

<sup>1</sup>Dipartimento di Fisica, Informatica e Matematica, Università di Modena e Reggio Emilia, Modena, Italy; <sup>2</sup>Ernst Ruska-Centre for Microscopy and Spectroscopy with Electrons, Forschungszentrum Julich, Julich, Germany; <sup>3</sup>CNR-Istituto Nanoscienze, Centro S3, Modena, Italy; <sup>4</sup>CNR-IMM, centro CNR, Bologna, Italy

E-mail: paolo.rosi@unimore.it

The Orbital Angular Momentum (OAM) sorter is a useful approach for the measurement of OAM for light<sup>1</sup>. The same device is now under study for electrons<sup>2-4</sup>. The prospect is that it is going to drastically change the measurement paradigm in electron microscopy.

We previously designed and implemented a working OAM sorting system by holographic means<sup>3</sup>. However, building an equivalent device based on electrostatic lenses is a very difficult task that requires modeling of fields and ray propagation in the microscope and design of MEMS devices. Due to its intrinsic higher efficiency with respect to the holographic approach, *i.e.* less “useful” electrons are lost in the sorting process, it pays off in its application in measuring plasmon resonances<sup>5</sup>, magnetization properties of materials<sup>6</sup> and proteins structures<sup>7</sup>.

The electrostatic OAM sorter devices have been realized on MEMS chips by means of optical lithography at the CNR-IMM institute in Bologna. Once fabricated, the devices have been polished and reshaped by FIB milling to remove leftovers from the etching process and achieve the desired tip shape. Finite elements simulations have been carried out, alongside analytical calculations, to design the best performing device (Figure 1.a and b).

By means of electron holography we measured the phase shift produced by the sorting objects (Figure 2a and b).

From simulation in the ideal working conditions, the electrostatic phase plates that we designed should reach an OAM resolution of 1  $\hbar$ , and indeed already in preliminary experiments, where not all the parameters have been perfectly tuned, we have been able to achieve an OAM resolution of about 1.5 to 2  $\hbar$ .

In conclusion, here we show the promising experimental and theoretical results toward the realization of an OAM sorter to be introduced inside an electron microscope. The device promises to be an important advance in electron microscopy and to improve our understanding of plasmonic and magnetic structure.

Figure 1. a) and b) show the modelled tip design and the phase of the central tip calculated by finite elements; c) shows the ideal phase of a charged, point like tip; d) and e) are SEM images of the electrostatic sorter devices, namely S1 and S2 respectively. f) and g) show the experimental phase of the two sorting elements, respectively S1 and S2; while h) and i) show the ideal phase of the two.

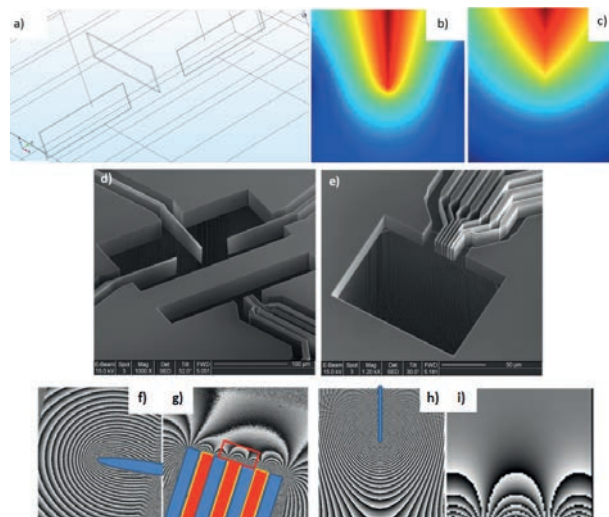


**Figure 1.** a) and b) show the modelled tip design and the phase of the central tip calculated by finite elements; c) shows the ideal phase of a charged, point like tip; d) and e) are SEM images of the electrostatic sorter devices, namely S1 and S2 respectively. f) and g) show the experimental phase of the two sorting elements, respectively S1 and S2; while h) and i) show the ideal phase of the two.

### References

1. Berkhout GC, et al. Phys Rev Lett 2010, 105:153601.
2. McMorran B, et al. New J Phys 2017, 19:023053.
3. Grillo V, et al. Nature Comm 2017, 8:15536.
4. Pozzi G, et al. <https://arxiv.org/abs/1906.02344>
5. Zanfrognini M, et al. ACS Photonics 2019, 6.3, 620-7
6. Rotunno E, et al. <https://arxiv.org/abs/1905.08058>
7. Q-SORT 2019 International Conference abstracts

## HOTOMOGRAPHIC MICROSCOPE AS A NEW APPROACH FOR MONITORING APOPTOTIC CELL

S. Salucci<sup>1</sup>, M. Battistelli<sup>1</sup>, F. Sbrana<sup>2</sup>, D. Burini<sup>1</sup>, S. Burattini<sup>1</sup>, P. Giovanninetti<sup>2</sup>, E. Falcieri<sup>1</sup>

<sup>1</sup>Department of Biomolecular Sciences, University of Urbino Carlo Bo, Urbino, Italy; <sup>2</sup>IBF-CNR (Schaefer South-East Europe Srl), Genua Italy,

E-mail: sara.salucci@uniurb.it

Apoptosis, the main cell death process, plays crucial roles in normal and pathological conditions. It is essential for embryogenesis, tissue homeostasis and organ development. On the other hand, its deregulation can induce carcinogenesis and cancer progression. It can be triggered by a variety of stimuli and it is routed through two main pathways, the extrinsic and the intrinsic one. From a morphological point of view it is characterized by specific features which include cell shrinkage, blebbing, chromatin condensation, as well as micronuclei and apoptotic body presence<sup>1</sup>.

All these ultrastructural patterns have been described by means of conventional electron microscopy, which requires chemical fixation, staining and long time of sample preparation<sup>2</sup>. To limit these disadvantages, researchers have developed a new Holotomographic Microscope (HT), which through optical diffraction tomography, is able to investigate and monitor the morphological changes which occur in biological systems. Here, U937 haematopoietic cells, exposed to camptothecin treatment, able to trigger apoptotic cell death, have been analysed *in vivo* with HT<sup>3</sup>. 3D holotomographic images show the three-dimensional distribution of cell components, and reveal a clear ultrastructure preservation in control condition (Figure 1A, B), where the cells present a typical roundig shape with a large central nucleus, already observed and described through conventional microscopies.<sup>1</sup>

In cells exposed to camptothecin drug, the classical features of programmed cell death are easily detectable, in par-

ticular blebbing and micronuclei presence (Figure 1C, D).

In conclusion, HT, if compared to other conventional electron microscopical approaches, can be considered suitable to analyze by an ultrastructural point of view, in a rapid way and in real time, cell response to various stimuli without any labeling, staining and coating.

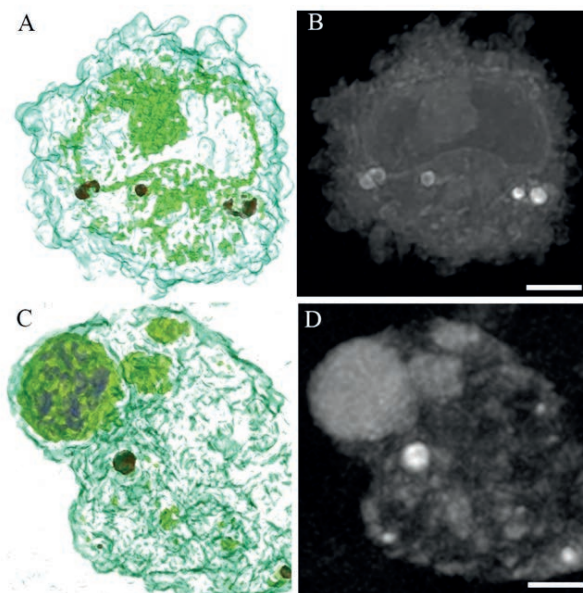


**Figure 1. Control (A,B) and treated (C,D) U937 cells observed at holotomographic microscope. Bars: 2  $\mu$ m.**

### References

1. Salucci S, et al. *Int J Mol Sci*. 2014, 15: 6625-40
2. Salucci S, et al. *Eur J Histochem*. 2018, 62:2881.
3. Salucci S, et al. *Eur J Histochem* 2019, 63(Suppl 2):29.